JOURNAL OF VIROLOGY, Apr. 1995, p. 2366–2377 Vol. 69, No. 4
0022-538X/95/$04.00+0

Sequence Requirements for Encapsidation of Deletion Mutants and Chimeras of Human Immunodeficiency Virus Type 1 Gag Precursor into Retrovirus-Like Particles

CHRISTIAN CARRIÈRE, BERNARD GAY, NATHALIE CHAZAL, NATHALIE MORIN, AND PIERRE BOULANGER*

Faculté de Médecine, Laboratoire de Virologie et Pathogénèse Moléculaires (CNRS URA-1487), Institut de Biologie, 34060 Montpellier, France

Received 21 July 1994/Accepted 5 January 1995

Interacting domains in human immunodeficiency virus type 1 (HIV-1) Gag precursor ($Pr55^{gag}$) expressed in recombinant baculovirus-infected cells were investigated by three different methods: (i) *trans* rescue and coencapsidation of C-terminal deletion (amber) Gag mutants and Gag chimeras into retrovirus-like particles in complementation experiments with HIV-1 wild-type (WT) $Pr55^{gag}$, (ii) Gag-Gag interactions in vitro in Gag ligand affinity blotting assays, and (iii) quantitative immunoelectron microscopy of retrovirus-like Gag particles, using a panel of monoclonal antibodies to probe the epitope accessibility of encapsidated HIV-1 WT $Pr55^{gag}$. Four discrete regions, within residues 210 to 241, 277 to 306 (major homology region), and 307 to 333 in the capsid (CA) protein and residues 358 to 374 at the CA-spacer peptide 2 (sp2) junction, were found to have a significant influence on Gag *trans*-packaging efficiency. A fifth region, within residues 375 to 426, overlapping the sp2-nucleocapsid (NC) protein junction and most of the NC, seemed to be essential for stable inter-Gag binding in vitro. The coincidence of the two regions from 358 to 374 and 375 to 426 with an immunologically silent domain in WT Gag particles suggested that they could participate in direct Gag interactions.

The morphogenetic pathway of human immunodeficiency virus type 1 (HIV-1) essentially follows that of type C retroviruses, characterized by the simultaneous assembly and budding of Gag particles at the plasma membrane (15, 61). HIV-1 Gag precursor is a polyprotein of 55 kDa ($Pr55^{gag}$), composed of four major and two minor structural domains, defined by the viral protease cleavage sites (20, 34). The major domains consist of the N-myristylated p17 matrix (MA) protein, the phosphorylated p24 capsid (CA) protein, the p7 RNA-binding nucleocapsid (NC) protein, and the p6 C-terminal domain. The two minor domains are spacer peptides localized at the CA-NC junction (sp2) and at the NC-p6 junction (sp1), respectively (20). These domains and their specific signals are sketched in Fig. 1.

HIV-1 wild-type (WT) $Pr55^{gag}$ expressed by recombinant baculovirus in insect cells has been found to be released in significant amounts into the external medium as membrane-enveloped, retrovirus-like particles of 100 to 130 nm in diameter (16, 22, 37, 42, 43). *N*-myristyl modification at the N terminus of the MA domain of HIV-1 $Pr55^{gag}$ is indispensable for the budding process (16, 42, 43) as well as for infectious virus particle production by mammalian cells (4, 18, 38). However, unmyristylated Gag and Gag-Pol polyproteins of HIV-1 (21, 39, 46) and membrane-binding mutants of Rous sarcoma virus (RSV) (60, 62) can be efficiently copackaged into retroviral particles by WT Gag precursor coexpressed in *trans*. In contrast, unmyristylated $Pr65^{gag}$ of Moloney murine leukemia virus has been shown to be excluded from the virus assembly process (40, 45).

The domains which are critical in *cis* for transport, self-assembly, and budding of HIV-1 Gag particles have been extensively studied by using deletion, insertion, and substitution mutagenesis of $Pr55^{gag}$ (6, 10, 11, 13, 16, 17, 21, 24, 31, 47, 52, 53, 55, 63–67) or inhibition of virus particle formation by synthetic peptides mimicking Gag sequences (35). However, mutational analysis rarely allows one to discriminate between direct and indirect effects of a mutation and distinguish whether an assembly-defective phenotype results from a mutated residue in interacting domains or from a mutation-induced overall change in the protein conformation.

In this study, the domains required in *trans* for HIV-1 Gag intermolecular interaction and coencapsidation were investigated by using three different approaches. (i) In vivo, the capacity of carboxy-terminally deleted (amber) Gag mutants and Gag chimeras to be *trans* rescued and coencapsidated by WT Gag was assayed in complementation with recombinant HIV-1 WT $Pr55^{gag}$ coexpressed in the same insect cells. (ii) In vitro, the affinity of Gag amber mutants for WT $Pr55^{gag}$ was assayed by protein blotting, using soluble Gag protein as the ligand. (iii) Homogeneous retrovirus-like Gag particles composed of WT $Pr55^{gag}$, and composite Gag particles containing both WT $Pr55^{gag}$ and chimeric Gag molecules, were probed for epitope accessibility and examined in quantitative immunoelectron microscopy (QIEM). Taken together, the results suggested that three discrete regions in the CA, including the cyclophilin-binding domain (30) and the major homology region (MHR) (61), the spacer peptide sp2, and the portion of the NC domain overlapping the two cysteine-histidine boxes played a significant role in Gag interaction.

MATERIALS AND METHODS

Cells and virus infection. IPLB-Sf21-AE (Invitrogen Corp., San Diego, Calif.), an Sf9 subclone of *Spodoptera frugiperda* cells, was maintained as monolayers at 28°C in Grace's insect medium (Sigma) supplemented with 10% fetal calf serum (Gibco) and Yeastolate and lactalbumin hydrolysate at 3.3 g/liter each. They

* Corresponding author. Mailing address: Laboratoire de Virologie & Pathogénèse Moléculaires, Institut de Biologie, Faculté de Médecine, 34060 Montpellier Cedex, France. Phone: (33) 67 60 57 38. Fax: (33) 67 54 23 78. Electronic mail address: boulange@arthur.citi2.fr.

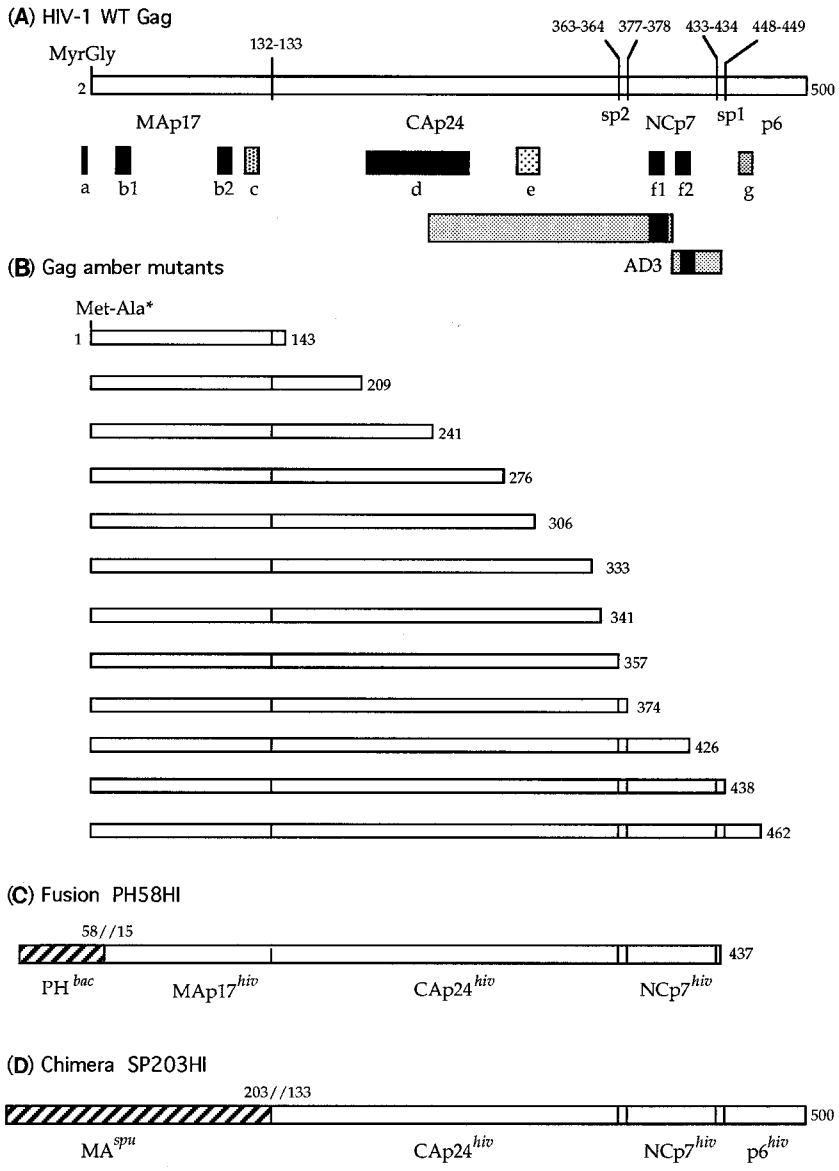

FIG. 1. Schematic diagrams of Gag proteins. (A) HIV-1 WT Pr55^{gag}. The major domains (MA, CA, NC p7, and p6) and spacer peptides sp2 and sp1, defined by the HIV-1 protease cleavage sites (small vertical bars), are shown on the Gag precursor linear sequence and numbered from the initiation Met-1 of the HIV-1$_{LAV}$ Gag sequence (54). Black and stippled boxes mark the positions of the following sequence elements: a, myristylated N terminus; b1 and b2, polybasic motifs at residues 26 to 32 and 110 to 114 in the MA; c, decapeptide ^{119}AADTGHSSQV^{128}, conserved in structural proteins of nonrelated RNA viruses (3); d, cyclophilin-binding region (210 to 267) (30); e, MHR, within residues 285 to 304 (61); f1 and f2, His-Cys boxes at positions 392 to 405 and 413 to 426, respectively; g, conserved PTAPP sequence, at positions 455 to 459 in p6; and AD3, the third major assembly domain of retrovirus Gag, composed of two subdomains, 241 to 407 and 408 to 437 (2, 60, 61). (B) Carboxy-truncated Gag amber mutants. The Gly-to-Ala substitution at position 2 generates the unmyristylated configuration. Each number on the right indicates the last residue of the Gag sequence preceding the amber stop codon. (C and D) Gag chimeras, with foreign sequences indicated by hatched boxes. In PH58HI, the N-terminal 58 residues from the baculovirus polyhedrin sequence were fused to Arg-15 of the HIV-1 MA. In SP203HI, the entire HSRV MA (203 residues) was substituted for the HIV-1 MA. *bac*, baculovirus; *hiv*, HIV; *spu*, spumaretrovirus.

were infected at a multiplicity of infection (MOI) ranging from 5 to 15 PFU per cell. In coinfection experiments, in which equal production of two recombinant Gag proteins coexpressed in *trans* was needed, cell samples were simultaneously infected by the two recombinant baculoviruses, WT and mutant, at various MOI ratios, e.g., 5:2.5, 5:5, 5:7.5, 5:10, and 5:12.5 PFU per cell. Cell lysates were quantitatively assayed for double Gag expression (see below), and the infected cell sample giving equivalent signals for both recombinant Gag was retained.

Construction of recombinant Gag mutants and chimeras. The baculovirus transfer vector used in this study, pGmAc115T-N, had the polyhedrin start codon A(+1)TG mutated to ATT, as in pVL941 (32), a *Bgl*II-*Nco*I linker inserted at nucleotide +34, and an *Xba*I linker at position +407 in the polyhedrin coding sequence. Cloned genes were thus expressed under the control of the polyhedrin promoter. The entire nucleotide sequence of HIV-1$_{LAV}$ *gag* gene (54), modified at its 5′ extremity to generate an *Nco*I site including its ATG initiation codon, was inserted between the *Nco*I and *Xba*I sites, generating pGmAc-NGag. All genetic constructs and mutations in the HIV-1 *gag* gene were first made in two derivatives of the pBluescript II KS− plasmid containing the *gag* coding sequence and starting its ATG initiator at an *Nco*I site. Their 5′-end sequence provided the two possible N termini for the recombinant Gag mutants, N myristylated, as in WT Pr55^{gag} (Gag12myr+) (42, 43), or unmyristylated, as in N-myristylation-defective mutant GagG2A (6, 7). Mutation-containing fragments were excised by restriction digestion with two unique sites on each side of the mutation and replaced into the same sites of pGmAc-NGag. The oligonucleotides required for mutagenesis or cloning strategies were synthesized by Eurogentec (Seraing, Belgium). Recombinant baculoviruses were obtained by in vivo recombination in Sf9 cells between pGmAc-NGag and *Bsu*36I-digested DNA from *Autographa californica* nuclear polyhedrosis virus (AcNPV)-derived BacPAK6 virus (Clonetech Laboratories, Palo Alto, Calif.).

Deletion mutant *amb*143 consisted of the MA domain and 11 amino acids from the CA (7). The other carboxy-truncated mutants of recombinant Gag precursor were constructed by insertion of an amber multistop codon (double-stranded 5′-CTAGTCTAGACTAG-3′ *Xba*I linker) into the blunted *Eco*RI site created at *gag* codons 209, 241, 334, 341, 357, 374, 426, 438, and 462 by our linker-insertion mutagenesis (6). They are referred to as *amb*209, *amb*241, *amb*333, *amb*341, etc. The number refers to the last residue of the Gag sequence, regardless of foreign amino acids introduced by the cloning sites and multistop oligonucleotide, and in designations such as *amb*143myr+ or *amb*462myr−, the suffix myr+ or myr− indicates to the N-terminal modification. Mutants *amb*276 and *amb*306 were generated by PCR amplification, using primer pairs A and B or A and C, sense and antisense, respectively. Oligonucleotide A (5′-CTGGGA CAGCTACAACCATCC-3′) corresponded to the sequence between codons 61 and 67 of *gag*. Primer B (5′-GCTCTACATTCTTACTATTTTATT-3′), from codons 278 to 271, introduced a mismatch at codon 277, changing the tyrosine to an amber stop codon. Primer C (5′-TTGCTAGGCTCTTAGAGTTTTATA-3′), corresponding to *gag* codons 306 to 301, introduced a Glu-to-amber change at position 307. The PCR fragments were cloned into pBluescript II KS−, verified by DNA sequencing, then excised by digestion at the unique sites *Pst*I (codon 210 in *gag*) and *Kpn*I in the cloning cassette, and reintroduced between the same unique sites of pGmAc-NGag baculoviral vector.

The construction and phenotype of the AcNPV polyhedrin–HIV-1 Gag fusion protein (Gag5) have been described elsewhere (42, 43). Gag5 consists of the p6-sp1-deleted Gag precursor, terminated at codon 437 in the NC sequence (*Bgl*II site) and fused to the N-terminal 58 amino acids from the baculoviral polyhedrin. To standardize our nomenclature, it is now termed PH58HI. The human spumaretrovirus (HSRV)–HIV-1 Gag chimera SP203HI consisted of the MA domain from HSRV (203 residues) linked to the 378 residues from the HIV-1 CA-NC domains. The HSRV genome, cloned as proviral DNA in pAT153 (29), was obtained from R. Flügel. HSRV *gag* gene was recovered by PCR amplification between primers D and E and subcloned into the *Sma*I site of pBluescript II KS−, generating pBKS-SpuGag. Oligonucleotide D (sense) corresponded to nucleotides (nt) 1200 to 1222 in the HSRV *gag* sequence (29) and introduced an *Eco*RI site upstream to the ATG at position 1223 (5′-CCGAATTCAGGCATATAAAAGCCAATAGACA-3′), whereas antisense E (nt 3121 to 3142, 5′-CCAAGCTTGGCTGTAACAGCTGAAGAGGAT-3′) inserted an *Hin*dIII site a few nucleotides upstream to the stop codon of HSRV *gag* (nt 3167). For construction of the SP203HI chimera, a *Bst*EII site, naturally present at the MA-CA junction of the HSRV Gag precursor, was created by PCR at the MA-CA junction of HIV-1 Gag. The HIV-1 CA-NC domain was amplified between primer F (nt 732 to 753, 5′-GCCCGGTTACCTATAGTGCAGAA CATCCAGG-3′), introducing the *Bst*EII site, and the antisense primer G (nt 1838 to 1820, 5′-CCCTCGAGTTATTGTGACGAGGGGTCG-3′), introducing an *Xho*I site downstream to the HIV-1 *gag* natural TAA stop codon at position 1836. The HIV-1 *gag* *Bst*EII-*Xho*I fragment was reinserted into the same unique sites of pBKS-SpuGag in place of the HSRV CA-NC domains. The chimeric *gag* gene was then excised by digestion by *Bgl*II-*Kpn*I and reinserted into *Bgl*II-*Kpn*I-digested pGmAc115T-N baculoviral transfer vector. The genomes of all mutants were verified by DNA sequence analysis, using the dideoxynucleotide chain termination technique (44) and the Sequenase kit, version 2.0 (U.S. Biochemical Corp., Cleveland, Ohio). The schematic diagrams of our Gag amber mutants and Gag chimeras are represented in Fig. 1.

Biochemical and immunological analyses. Retroviral Gag particles released from the plasma membrane of Sf9 cells were analyzed by ultracentrifugation in velocity gradient as already described (43). Sodium dodecyl sulfate (SDS)-denatured proteins were analyzed by SDS-polyacrylamide gel electrophoresis (PAGE) in 12.5% acrylamide gels (acrylamide-to-bisacrylamide ratio of 50:0.8), using a discontinuous buffer system (26). Electric transfer of proteins onto nitrocellulose membranes (Hybond-ECL; Amersham) was carried out in 25 mM Tris–192 mM glycine buffer (pH 8.3) containing 20% methanol at 0.8 mA/cm^2 for 90 min, using a semidry system (Cambridge Electrophoresis, Cambridge, United Kingdom). Blots were blocked with 5% skimmed milk and 1% calf serum in TBS-T buffer (20 mM Tris-HCl [pH 7.8], 0.15 M NaCl, 0.05% Tween 20) and then successively reacted with primary antibody and phosphatase-labeled or horseradish peroxidase-labeled anti-immunoglobulin G (IgG) conjugate. The following primary antibodies were used in immunoblotting: (i) HSRV-MA antiserum, raised in a rabbit by injection of glutathione *S*-transferase-fused, bacterially expressed (pGEX-KG [19]) HSRV matrix domain (amino acid residues 1 to 203), purified by affinity chromatography, preparative SDS-gel electrophoresis, and electroelution (Elutrap BT 1000; Schleicher & Schuell, Dassel, Germany); (ii) rabbit serum directed against AcNPV polyhedrin (laboratory made); (iii) rabbit serum against HIV-1 WT Pr55^{gag} (laboratory made); (iv) mouse anti-Pr55-p17 monoclonal antibody (MAb) Epiclone-5003 (Epitope, Beaverton, Ore.), and (v) mouse anti-Pr55-p24 MAb Epiclone-5001. All antibodies were used at a dilution of 1:1,000. Color development was performed with 5-bromo-4-chloro-3-indolyl phosphate toluidinium and nitroblue tetrazolium (Boehringer). Immunological quantification of proteins was carried out as previously described (7), using a chemiluminescent peroxidase substrate (Luminol; Amersham). Luminograms (Hyperfilm-ECL; Amersham) were scanned at 610 nm, using an automatic densitometer system (REP-EDC; Helena Laboratories, Beaumont, Tex.). Ligand affinity blotting (9, 36) was performed like immunoblotting except that the primary antibody was replaced by a Gag solution (0.1 mg/ml in TBS-T), with overnight incubation at room temperature. Bound Gag ligands were detected by their specific epitope tags: the M35/2F8 MAb epitope in the p6 carboxy-terminal domain of full-length Pr55^{gag} when amber Gag mutants were immobilized on blots and Pr55^{gag} was used as the ligand (7, 51), or the Epiclone-5001 epitope, destroyed in the insertion mutant *in*341 (6), when *in*341 Gag was immobilized on blots and amber Gag mutants were used as the ligands.

EM and QIEM. For conventional electron microscopy (EM), Sf9 cells infected at an MOI of 10 PFU of Gag recombinant per cell were harvested at 48 h postinfection. The cell pellets were fixed with 2.5% glutaraldehyde in 0.1 M phosphate buffer (pH 7.5), postfixed with osmium tetroxide (2% in H_2O), and treated with tannic acid (0.5% in H_2O). After dehydration, the specimens were embedded in Epon (Epok-812; Fullam, Latham, N.Y.). Sections were stained with 2.6% alkaline lead citrate and 0.5% uranyl acetate in 50% ethanol. For QIEM with single or double immunogold labeling, cell specimens were embedded in hydrophilic metacrylic resin (Lowicryl K4M; Chemische Werke Lowi, Waldkraiburg, Germany), and sections reacted with antibody diluted in Tris-buffered saline overnight at 4°C. Secondary antibody reaction was carried out at room temperature for 1 h, using anti-mouse, anti-rat, or anti-rabbit IgG antibodies (diluted at 1:50 in Tris-buffered saline) labeled with 5-nm or 10-nm colloidal gold particles (EM-GAM5 or EM-GAM10; BioCell Research Laboratories, Cardiff, United Kingdom). Sections were stained with 2% uranyl acetate in H_2O and examined under a Hitachi-H7100 electron microscope.

Of the 17 anti-Gag MAbs used in our QIEM study, 12 have been analyzed in immunocapture enzyme-linked immunosorbent assay against synthetic peptides, and their epitopes have been mapped in the Pr55^{gag} sequence (41). The epitope recognized by MAb Epiclone-5003 has been localized between residues 120 and 132 in p17, using Gag deletion mutants (7). The epitope recognized by MAb Epiclone-5001 has been previously found to be destroyed by insertions at positions 334 and 341 in p24 (6). Gag mutant *amb*341, constructed in this study, failed to react with Epiclone-5001, whereas *amb*357 still did, which mapped the Epiclone-5001 epitope to between residues 341 and 357 in p24. Likewise, rat MAb M35/2F8, obtained from M. G. Sarngadharan (51), was mapped to between residues 463 and 500 in the p6 domain, since it reacted with WT Pr55^{gag} and not with *amb*462 mutant. Mouse anti-p7NC MAb HH3 (49) was obtained from R. Benarous, and rat anti-p7NC MAb i5B11 (5) was obtained from M. Bodeus. The characteristics of the MAbs used in QIEM and the positions of their epitopes are listed in Table 2. A mouse MAb against native adenovirus penton base (6B2 [25]) was used as the negative control for background labeling. All MAbs were first tested in immunoblotting assays and were found to react against Pr55^{gag} at dilutions ranging from 1:500 to 1:1,000. They were used in QIEM at a 100-fold-higher concentration, i.e., 1:10 to 1:5. To obtain statistically significant values, several hundreds of retroviral Gag particles were examined in immunogold labeling with each MAb, and gold grains were counted with a dissection microscope (36). The histogram of distribution of gold grains per Gag particle was determined for each MAb.

RESULTS

***trans* rescue and coencapsidation of carboxy-truncated Gag (amber) mutants.** To determine the sequence requirements for *trans* rescue of HIV-1 Gag mutants by WT Pr55^{gag} and coencapsidation into retrovirus-like particles, Sf9 cells were coinfected with Gag12myr+, expressing N-myristylated WT Pr55^{gag}, and a second recombinant expressing a Gag mutant in its N-myristylated or unmyristylated configuration. Stop codons introduced into the CA domain of HIV-1 Pr55^{gag} generated a panel of 12 Gag amber mutants with progressively shorter *gag* open reading frames, from *amb*462, truncated in its p6 domain, to *amb*143, truncated near the MA-CA junction (Fig. 1). Gag particles released into the culture medium of coinfected cells were analyzed by ultracentrifugation in a velocity gradient, SDS-PAGE, and immunoblotting. Gag proteins of mutants *amb*462myr−, *amb*438myr−, *amb*426myr−, *amb*374myr−, *amb*357myr−, *amb*341myr−, *amb*333myr−, and *amb*306myr− were rescued in *trans* by WT Pr55^{gag} and were detected in extracellular Gag particles. By contrast, there was no detectable coencapsidation for mutants *amb*276myr−, *amb*241myr−, *amb*209myr−, and *amb*143myr− (Fig. 2 and Table 1). This result implied that deletion of the sequence between amino acids 277 and 306 was detrimental to coincorporation of unmyristylated Gag precursor into budding particles.

The N-myristylated versions of the Gag amber mutants were also analyzed in *trans*-rescue assays with WT Pr55^{gag}. However, certain N-myristylated HIV-1 Gag carboxy-truncated mutants

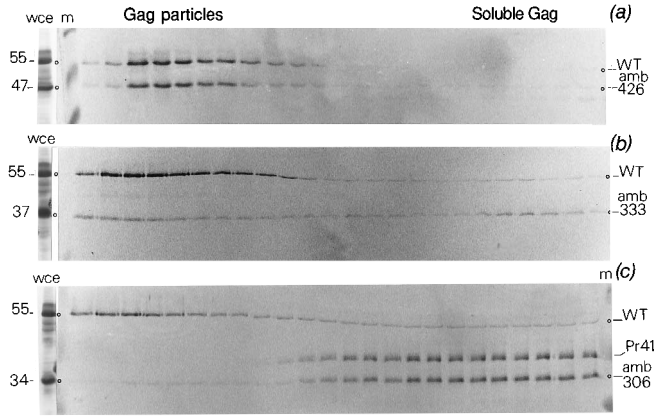

FIG. 2. *trans* rescue of unmyristylated Gag amber mutants analyzed by ultracentrifugation in a velocity gradient. Culture medium samples of cells coinfected with Gag12myr+ (WT Pr55^{gag}) and *amb*426myr− (a), *amb*333myr− (b), or *amb*306myr− (c) were harvested at 48 h postinfection, and extracellular Gag particles released by budding were analyzed in a sucrose gradient. Aliquots from the gradient fractions were analyzed by SDS-PAGE and immunoblotting with anti-Pr55-p17 MAb Epiclone-5003 and phosphatase-labeled conjugate. wce, control lane showing whole cell extracts from coinfected cells; m, marker lane. The positions of WT Pr55^{gag} and Gag amber mutants and their apparent molecular masses (55, 47, 37, and 34 kDa, respectively) are indicated by dots on both sides of the blots. Pr41^{gag}, visible in the fractions containing soluble Gag, corresponds to a major Gag precursor cleavage product (p17-p25 domains). Note the difference in coencapsidation efficiency between *amb*426myr− (high) and *amb*333myr− and *amb*306myr− (low), as detailed in Table 1.

present a WT budding phenotype, and in contrast to mammalian cells (17), baculovirus-infected insect cells have the capacity to support the budding and extracellular release of p6-deleted recombinant Gag precursor (42, 43). Thus, *trans*-rescue assays could not be performed with amber mutants located on the C-terminal side of the boundary for particle budding capacity, recently identified at the sp2-NC junction in baculovirus-expressed HIV-1 Gag (24). This investigation was therefore restricted to the nine budding-defective mutants, *amb*143myr+, *amb*209myr+, *amb*241myr+, *amb*276myr+, *amb*306myr+, *amb*333myr+, *amb*341myr+, *amb*357myr+, and *amb*374myr+. All of these N-myristylated amber mutants were found to be coencapsidated by WT Pr55^{gag}, although to various extents (Table 1).

TABLE 1. Coencapsidation efficiency[a] of HIV-1 Gag amber mutants and Gag chimeras in coexpression with HIV-1 WT Pr55^{gag}

Recombinant	Coencapsidation efficiency (%)[b]	
	N-myr+	N-myr−
Carboxy-truncated Gag		
*amb*143	4.3 ± 2.9	ND[c]
*amb*209	9.4 ± 3.0	ND
*amb*241	15.3 ± 3.2	ND
*amb*276	17.1 ± 7.4	ND
*amb*306	23.7 ± 3.5	2.9 ± 0.76
*amb*333	40.0 ± 2.3	16.7 ± 3.53
*amb*341	44.5 ± 5.9	6.9 ± 0.71
*amb*357	44.0 ± 7.3	8.9 ± 0.45
*amb*374	47.5 ± 3.0	31.2 ± 0.94
*amb*426[d]		40.8 ± 0.20
*amb*438[d]		35.2 ± 2.59
*amb*462[d]		38.1 ± 1.88
Chimeric Gag (unmyristylated)		
PH58HI		28.2 ± 5.6
SP203HI		15.0 ± 5.5

[a] Sf9 cells were coinfected with equal MOIs of two recombinants, one expressing WT Pr55^{gag} (Gag12myr+) the other expressing a Gag chimera or an amber Gag mutant in its N-myristylated (N-myr+) or unmyristylated (N-myr−) configuration. Membrane-enveloped virus-like particles released at 48 h postinfection were immunologically assayed for Gag protein content.

[b] Estimated from the amount of Gag amber mutant or Gag chimera found in composite particles, expressed as the percentage of total Gag polyprotein (± standard deviation; $n = 5$ for amber mutants; $n = 10$ for Gag chimeras).

[c] ND, not detected.

[d] For the N-myristylated Gag amber mutants with a WT budding phenotype, coencapsidation with WT Pr55^{gag} could not be assessed.

The efficiency of coencapsidation, estimated from the ratio of amber mutant to WT Gag signals in luminograms of immunoblotted Gag particles, showed two thresholds in the coencapsidation level of unmyristylated Gag mutants: one between *amb*276myr− and *amb*306myr− and one between *amb*357myr− and *amb*374myr−. Mutants *amb*143myr−, *amb*209myr−, *amb*241myr−, and *amb*276myr− showed no detectable coencapsidation. Mutants *amb*306myr−, *amb*333myr−, *amb*341myr−, and *amb*357myr− were found to be coencapsidated at relatively low levels (3 to 16%), whereas in *amb*374myr−, *amb*426myr−, *amb*438myr−, and *amb*462myr−, coencapsidation occurred at levels ranging from 30 to 40%. In the N-myristylated series, two thresholds could also be distinguished, with a twofold increase in copackaging efficiency between mutants *amb*209myr+ and *amb*241myr+ and between *amb*306myr+ and *amb*333myr+ (Table 1).

Gag interaction in vitro. The domains required for in vitro interaction and stable binding between Gag precursor molecules were investigated by ligand affinity blotting assays. In assay 1, unmyristylated Gag amber mutants analyzed by SDS-PAGE were immobilized on a membrane and soluble unmyristylated full-length Gag precursor expressed by mutant G2A, immunologically detectable by its p6 domain, was used as the ligand. The results are shown in Fig. 3. An intense signal of bound Gag was observed on blots for mutants *amb*462, *amb*438, and *amb*426. A faint signal of Gag ligand binding was still visible with *amb*374, *amb*357, *amb*341, and *amb*333, but no binding was detectable with shorter Gag amber mutants (*amb*306 to *amb*143). A possible influence of SDS denaturation and partial renaturation of immobilized Gag amber mutants on the efficiency and/or specificity of binding was examined by a reverse in vitro binding reaction (assay 2). Full-length Gag precursor was electrophoresed and transferred to the solid support, whereas soluble, nondenatured Gag amber mutants were used as the ligands. The blotted full-length Gag used was from *in*341myr−, an insertion mutant which has lost its reactivity toward MAb Epiclone-5001 (6). This allowed us to distinguish the bound Gag ligands *amb*462, *amb*438, *amb*426, *amb*374, and *amb*357, which all carried the Epiclone-5001 epitope, from the immobilized Gag species. The results obtained with the reverse Gag ligand affinity blotting assays (data not shown) were similar to those obtained with assay 1 and confirmed that the boundary between high- and low-affinity binding between Gag molecules in vitro lay between residues 375 and 426. This region corresponded to the sp2-NC junction and the portion of the NC domain overlapping the two zinc fingers.

Determinant accessibility in WT Gag particles analyzed by QIEM. Retrovirus-like particles released by budding from the plasma membrane of Sf9 cells expressing HIV-1 WT Pr55^{gag} (Gag12myr+) were probed with a panel of 17 characterized MAbs, and the accessibility of epitopes localized in different Gag domains was analyzed by EM. As shown in Fig. 4 and Table 2, the reactivities of particle-incorporated WT Pr55^{gag} varied from an average ratio of 29.5 colloidal gold grains per particle for the most highly reactive MAb RL4 (mapped be-

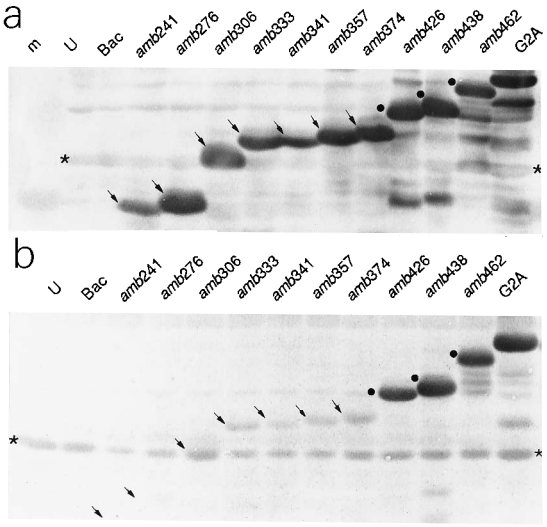

FIG. 3. Ligand affinity blotting assay, using Gag amber mutants immobilized on blot and full-length Gag precursor as the soluble ligand. In panel a, the control immunoblot was reacted with polyclonal anti-Pr55^{gag} rabbit antibody and phosphatase-labeled anti-rabbit IgG conjugate. In panel b, the affinity blot was incubated with soluble Gag ligand (p6-containing GagG2A), and Gag-Gag binding was detected by successive reactions with anti-p6 rat MAb and phosphatase-labeled anti-rat IgG conjugate. GagG2A, electrophoresed and transferred under the same conditions, was used as the positive control of anti-p6 reactivity (lane G2A). Immobilized Gag amber mutants which strongly bind to the Gag ligand (anti-p6 positive) are marked by black dots, whereas amber mutants faintly or not binding to the Gag ligand are indicated by arrows. m, marker lane; U, mock-infected cells; Bac, BacPAK6-infected cell extract. Asterisks indicate cellular background bands.

tween residues 219 and 233 in the CA domain) to 0.3 and 1.3 grains per Gag particle for the less reactive MAbs HH3 and i5B11, respectively. HH3 and i5B11 epitopes have been localized at both termini of the NC p7 domain, within residues 378 to 391 for i5B11 and residues 429 to 444 for HH3 (49). Both i5B11 and HH3 were highly reactive against isolated NC p7 and SDS-denatured Pr55^{gag} in immunoblotting (not shown), which suggested that their epitopes were buried and not accessible in encapsidated WT Pr55^{gag}. Five regions were thus found to be exposed in sectioned Gag particles: two at both extremities of the MA, within residues 11 to 25 and 113 to 132, two in the CA at positions 201 to 233 and 285 to 357, and one in the C-terminal moiety of the p6 domain (463 to 500). Both regions from 201 to 233 and 285 to 341 have already been identified as accessible and immunodominant regions in soluble CA protein (12, 27). These reactive regions delineated four silent windows: (i) within residues 26 to 112 in the MA, (ii) 133 to 200 and (iii) 234 to 284 in the CA, and (iv) a fourth zone within residues 357 to 462, overlapping the sp2, NC p7, and sp1 domains (Fig. 1 and Fig. 4). These inaccessible domains carried potential interacting sites between Gag precursor molecules.

***cis* effects of MA modifications on Gag interaction and assembly in vivo.** It was previously shown that the unmyristylated, polyhedrin-fused, p6-deleted Gag protein expressed by recombinant PH58HI in Sf9 cells was defective in extracellular budding of membrane-enveloped particles and was released as soluble protein into the culture medium (43). Likewise, the HIV-HSRV Gag chimera SP203HI, consisting of the unmyristylated HSRV MA fused to the HIV-1 CA-NC domains, was found to be released only as soluble protein, and no retrovirus-like particles were found at the plasma membrane of SP203HI-infected cells (data not shown). However, both PH58HI and SP203HI chimeras were capable of assembling core-like particles within the cell (Fig. 5). The intracellular particles made of p6-deleted, polyhedrin-fused PH58HI, or formed by the SP203HI chimera, were similar in size and morphology to the core particles composed of unmyristylated full-length HIV-1 Gag precursors expressed by Gag10 (42) or G2A (6). Their outer diameters in EM sections were 107.1 ± 4.7 nm for PH58HI (mean ± confidence interval at $P = 0.05$; $n = 31$) and 111.7 ± 5.1 nm for SP203HI ($n = 22$). This finding suggested that the fusion of the HIV-1 MA domain to foreign, nonretroviral sequence, as in PH58HI, or its complete replacement by another retroviral MA sequence, as in SP203HI, had no detrimental effects in *cis* on the intracellular assembly capacity of the resulting Gag chimeras. However, HIV-1 Gag insertion mutant *in*40 (6) and deletion mutant *dl*42-100 (7), which both accumulate a cleaved Gag species (Pr39^{gag}) lacking the MA domain, failed to assemble core structures within the cell, suggesting that the presence of an MA domain, homologous or heterologous, was essential for in vivo assembly of HIV-1 Gag precursor.

***trans* effects of MA modifications on Gag coencapsidation.** Sf9 cells were coinfected with two recombinants, one expressing HIV-1 WT Pr55^{gag} (Gag12myr+) and the other expressing an MA mutant or a Gag chimera, both Gag species being distinguishable by their unique epitope tags and/or apparent molecular masses in SDS-PAGE. Mutants *in*40 and *dl*42-100 showed no detectable *trans* rescue of their cleaved precursor Pr39^{gag} in coinfection with WT Pr55^{gag} (data not shown), suggesting that the presence of an MA domain, regardless of its *N*-myristyl modification, was indispensable for HIV-1 Gag precursor coencapsidation.

In cells coinfected by PH58HI and Gag12myr+, the budding-defective phenotype of PH58HI (42, 43) was efficiently rescued in *trans* by coexpressed WT Pr55^{gag}. SDS-PAGE and immunoblot analysis of the velocity gradient fractions corresponding to particulate Gag sedimenting at 600 to 700S (1.17 in apparent density) showed that the Gag particles released by coinfected cells were heterogeneous in nature and contained two Gag signals (Fig. 6a) that were electrophoretically and immunologically identifiable: the HIV-1 WT Gag precursor of 55 kDa reacted with anti-p6 MAb, whereas PH58HI (53 kDa), tagged at its N terminus by 58 amino acids from the polyhedrin sequence, lacked the p6 domain. An efficient complementation effect was also observed in coexpression of HIV-1 Pr55^{gag} and an unmyristylated Gag chimera SP203HI (65 kDa; Fig. 6c). As estimated from densitometric scanning of immunoblot luminograms, the *trans*-rescue efficiencies, expressed as the percentages of total Gag molecules coencapsidated, were 28% for PH58HI and 15% for SP203HI (Table 1).

The occurrence of composite retrovirus-like particles containing two different (N-myristylated and unmyristylated) Gag protein species was confirmed by immunoelectron microscopy. Gag particle reactivity was probed in EM sections of cells coinfected by Gag12myr+ and PH58HI or Gag12myr+ and SP203HI, using anti-p6 rat MAb and antipolyhedrin rabbit antibody for the first pair and anti-HIV p17 mouse MAb and anti-HSRV MA rabbit antibody for the second pair. Specific Gag epitopes were then distinguished on individual core particles by using differential labeling of the conjugate, i.e., 5-nm-colloidal gold-labeled anti-rat IgG and anti-mouse IgG antibodies and 10-nm-colloidal gold-labeled anti-rabbit IgG antibody. Most of the plasma membrane-budding Gag particles were found to carry double immunogold labeling in both types of coinfection experiments, Gag12myr+-PH58HI and Gag12myr+-SP203HI (Fig. 6b and d), thus confirming the results of biochemical analyses in sucrose gradients (Fig. 6a and c). The next analysis was designed to determine the influ-

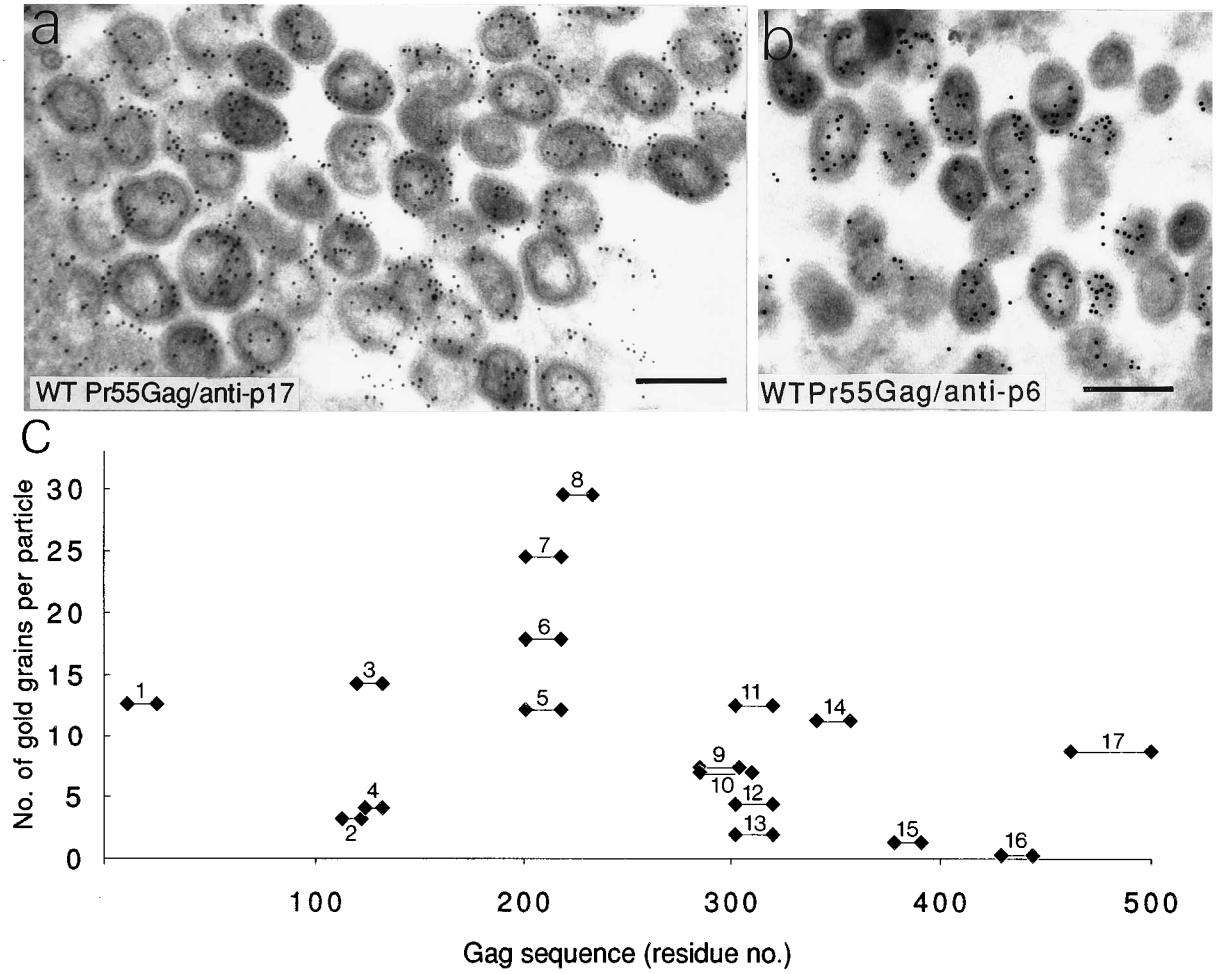

FIG. 4. Immunoreactivity of encapsidated WT Pr55^{gag} analyzed by QIEM in single immunogold labeling. Extracellular WT Gag particles budding from the plasma membrane of Gag12myr+-infected cells were immunoreacted with anti-p17 MAb Epiclone-5003 (a) or anti-p6 MAb M35/2F8 (b) followed by 5-nm-gold-labeled conjugate. Bar, 200 nm. (c) QIEM analysis of WT Gag particles probed with a panel of 17 MAbs, the epitopes of which are aligned on the Gag precursor sequence. MAbs are identified by number as indicated in Table 2. Statistical data are also presented in Table 2.

ence of the intracellular environment on the composition of heterogeneous Gag particles and the role of cellular compartments in Gag coencapsidation.

QIEM analysis of homogeneous and heterogeneous Gag particles in different cell compartments. Several hundred individual Gag particles budding from the plasma membrane or assembled within cells coinfected with Gag12myr+ and PH58HI or with Gag12myr+ and SP203HI were statistically analyzed by QIEM after double immunogold labeling as described above. The reactivity of composite Gag particles assembled in coinfected cells was then compared to that of homogeneous particles formed during single infections. The results are presented in Table 3. In single infections, the anti-p6 reactivity of Gag particles constituted of full-length Gag precursor varied slightly with the cellular compartment in which they accumulated, from 16.6 gold grains per particle at the plasma membrane (N-myristylated Gag12myr+) to 18.7 and 22.6 gold grains per particle in the cytoplasm and nucleus, respectively (unmyristylated G2A mutant). Composite Gag particles harboring WT Pr55^{gag} and PH58HI showed a lower p6 reactivity in the nuclear compartment, and a significant polyhedrin labeling was observed in membrane-enveloped particles budding from the plasma membrane (4.8 grains per particle; Fig. 6b). The ratio of anti-p6 to antipolyhedrin reactivity, which reflected both the accessibility of each Gag protein species and its molar ratio within the core particle, was found to be higher at the plasma membrane than in the cytoplasm and nuclei of cells coexpressing WT Pr55^{gag} and PH58HI. The difference was significant at the $P = 0.05$ level. It must be remembered that a nuclear localization signal (^{29}KNAKRKK^{35}) is present in the fused polyhedrin sequence of PH58HI. A similar effect was observed in cells coexpressing WT Pr55^{gag} and SP203HI, with a twofold-higher ratio of HIV p17 to HSRV MA reactivity in membrane-budding particles than in intracytoplasmic particles (Table 3). This finding suggested that the number of copies of unmyristylated Gag chimera significantly differed in extracellular and intracellular particles, with a ratio to HIV-1 WT Pr55^{gag} minimum in particles released by budding and maximum in particles accumulated within the cell.

DISCUSSION

Immature virions of retroviruses are physiologically heterogeneous in Gag composition. In the case of HIV-1, they are constituted of a majority of Pr55^{gag} molecules and a minority of

TABLE 2. Epitope reactivities of encapsidated WT Pr55^{gag} analyzed by QIEM

MAb[a]		Epitope localization[b]	Reactivity[c]	No. of particles analyzed
No.	Designation			
1	L14.17	11–25	12.62 ± 0.93	232
2	3H7	113–122	3.20 ± 0.26	345
3	Epiclone-5003	120–132	14.31 ± 0.82	281
4	31-11	124–132	4.06 ± 0.34	438
5	8D2	201–218	12.16 ± 0.94	245
6	8H7	201–218	17.85 ± 1.32	239
7	47-2	201–218	24.53 ± 1.44	215
8	RL4.72.1	219–233	29.55 ± 1.68	136
9	23A5G4	285–304	7.40 ± 0.58	253
10	M09.42.2	285–310	6.98 ± 0.60	294
11	9A4C4	302–320	12.52 ± 0.72	259
12	11C10B10	302–320	4.41 ± 0.34	380
13	11D11F2	302–320	1.95 ± 0.20	366
14	Epiclone-5001	341–357	11.26 ± 0.84	306
15	i5B11	378–391	1.33 ± 0.19	237
16	HH3	429–444	0.30 ± 0.05	582
17	M35/2F8	463–500	8.75 ± 0.60	236
18	Control[d]		0.11 ± 0.07	138

[a] All were from mice except for i5B11 and M35/2F8, which were from rats.
[b] Mapped in the HIV-1 Gag precursor sequence as indicated in Materials and Methods. Amino acid numbering starts from the methionine initiation codon in the HIV-1 *gag* gene sequence (54).
[c] Expressed as the number of gold grains per budding Gag particle. Values are means ± confidence interval at the $P = 0.05$ level.
[d] Performed with mouse monoclonal anti-adenovirus type 2 penton base (25) and 5-nm-gold-labeled anti-mouse IgG conjugate.

polyproteins Pr160$^{gag\text{-}pol}$ (28), which lack p6 since they result from a frameshift event occurring at the C terminus of the p7 domain (23). Retrovirus-like particles composed of two different recombinant Gag precursors coexpressed in the same Sf9 cell might represent a model system for studying the coencapsidation process. In the present study, we took advantage of the capacity of *trans* rescue by HIV-1 WT Pr55^{gag} of unmyristylated, budding-defective Gag and Gag-Pol precursors (21, 39, 46) to delineate the boundary at which Gag amber mutants of decreasing polyprotein lengths were no longer coencapsidated into retrovirus-like particles.

A panel of 12 HIV-1 Gag amber mutants in both unmyristylated and N-myristylated configurations was thus generated and assayed in coexpression with WT Pr55^{gag}. In the N-myristylated series, all Gag amber mutants tested were found to be coencapsidated to some extent, even *amb*143myr+, the sequence of which is reduced to the MA domain and a short stretch of 11 amino acids from the CA domain (Table 1). This finding implied that some interacting domains exist in the MA domain of the HIV-1 Gag precursor. Two discrete regions, 210 to 241 and 307 to 333, seemed to have a significant effect on the *trans*-packaging efficiency of N-myristylated Gag amber mutants (Table 1). The first region, 210 to 241, partially coincides with the cyclophilin-binding domain of Gag (210 to 267 [30]). The second one, 307 to 333, belongs to a domain previously identified as being critical for Gag self-assembly by insertion and substitution mutagenesis (6, 21). It contains the motif ^{317}MTETLxxQNA^{326}, conserved in structural proteins of many RNA viruses, and residue Cys-330, common to the CA proteins of HIV, simian immunodeficiency virus, equine immunodeficiency virus, human T-cell leukemia virus type I, and maedi-visna virus (1).

No *trans* rescue was detected for unmyristylated Gag amber mutants which lacked the CA region from 277 to 306 (Table 1), suggesting that the MHR (33, 48, 61) was essential for this process. Furthermore, the coencapsidation of MHR-containing amber mutants occurred with a higher efficiency with the addition of the downstream sequence from 358 to 374, overlapping the CA-sp2 junction. The deletion of the spacer nonapeptide at the CA-NC junction of RSV has been found to abolish virus infectivity without obvious effects on the assembly of the mutant Gag and its release from the transfected cells. The loss of virus infectivity provoked by the mutation was attributed to a subtle change in the organization of the internal components of the virion, as suggested by the detergent sensitivity of the mutant particles, possibly via a role of the spacer peptide in directing folding and/or oligomerization of the CA subunits within the capsid structure (8).

The in vitro binding assays, using immobilized Gag amber mutants and soluble full-length Gag ligand, showed a low level of Gag binding to mutants containing MHR and downstream CA sequence until position 374. The highest Gag binding was obtained with amber mutants *amb*426, *amb*438, and *amb*462 (Fig. 3), suggesting that the sequence from 375 to 426 was essential for the occurrence of stable Gag interaction. The same sequence was also found to be nonreactive in QIEM analysis of WT Gag particles budding from the plasma membrane of Gag12myr+-infected cells in EM sections (Fig. 4).

Five regions were found to be exposed in budding WT Gag particles, within residues 11 to 25 near the N terminus of the MA, 113 to 132 near the MA-CA junction, 201 to 233 and 285 to 357 in the CA, and the C-terminal moiety (463 to 500) of the p6 domain (Fig. 4 and Table 2). These regions delineated four antigenically silent windows in the Pr55^{gag} sequence, which represented potential interacting domains between Gag precursor molecules: (i) within residues 26 to 112 in the MA, (ii) 133 to 200 and (iii) 234 to 284 in the CA, and (iv) 358 to 462, overlapping the sp2, NC p7, and sp1 domains (Fig. 1 and 4). The position of the last two windows is consistent with the recent report that the minimal domain required for HIV-1 Gag polyprotein multimerization in the GAL4 two-hybrid system is the region from 240 to 434 (14).

A comparison of the data from QIEM analysis of WT Gag particles and from *trans* rescue of Gag amber mutants showed that the Gag regions from 210 to 241 and 307 to 333, which were found to be critical for the coencapsidation of N-myristylated Gag amber mutants, were superimposed with the two highly reactive domains from 201 to 233 and 285 to 357, respectively. For the unmyristylated Gag amber mutants, the critical region from 277 to 306 coincided with the reactive domain from 285 to 357, whereas the sequence from 358 to 374 coincided with the silent domain from 358 to 462 (Table 1 and Fig. 4). The region of the Gag sequence which was found to be essential for Gag-Gag interaction in ligand binding assays (375 to 426) was also included in the silent domain from 358 to 462. It could thus be hypothesized that the two discrete silent regions, 358 to 374, as defined by the *trans*-rescue experiments, and 375 to 426, as identified by in vitro Gag binding assays, would participate in direct Gag interactions with WT Pr55^{gag}, whereas exposed regions from 210 to 241, 277 to 306, and 307 to 333 would have an indirect, conformational function in inter-Gag binding. The finding that the MHR is immunologically exposed within the Gag particles assembled in vivo (Table 2 and Fig. 4), as well as in recombinant CA protein oligomers assembled in vitro (12), would thus imply a conformational rather than direct role in Gag assembly and budding. Our

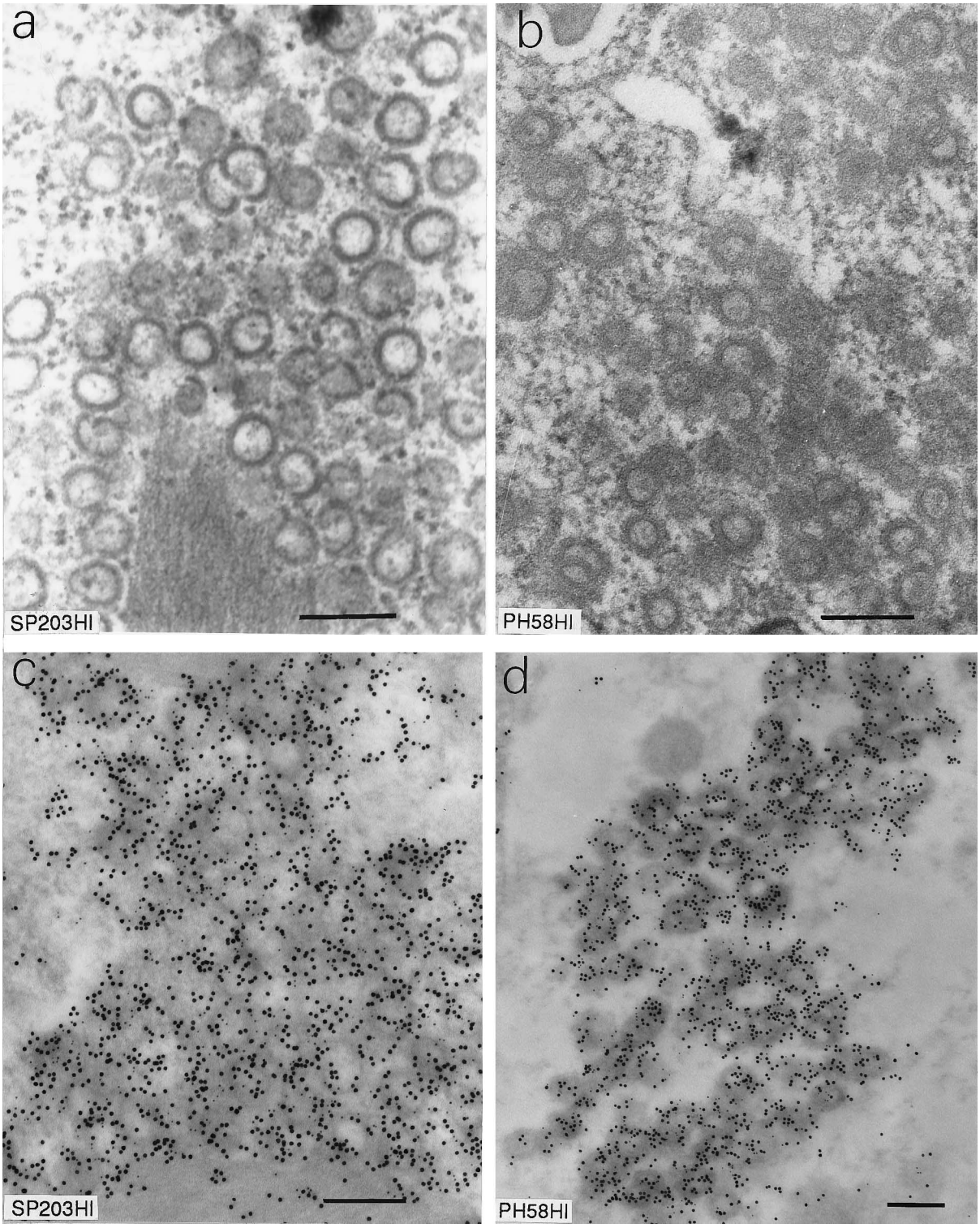

FIG. 5. Intracellular assembly of Gag chimeras in recombinant-infected Sf9 cells. (a and c) SP203HI, an HSRV-HIV chimera constituted of the MA domain of HSRV fused to the CA-NC domains of HIV-1. (b and d) PH58HI, a p6-deleted HIV-1 Gag precursor amino terminally fused to the N-terminal 58 residues from the polyhedrin sequence. (a and b) Conventional EM of osmium-fixed, Epon-embedded cell specimens; (c and d) IEM of Lowicryl-embedded cell sections, reacted with anti-HSRV MA antibody (b) or antipolyhedrin antibody (d). Bar, 200 nm.

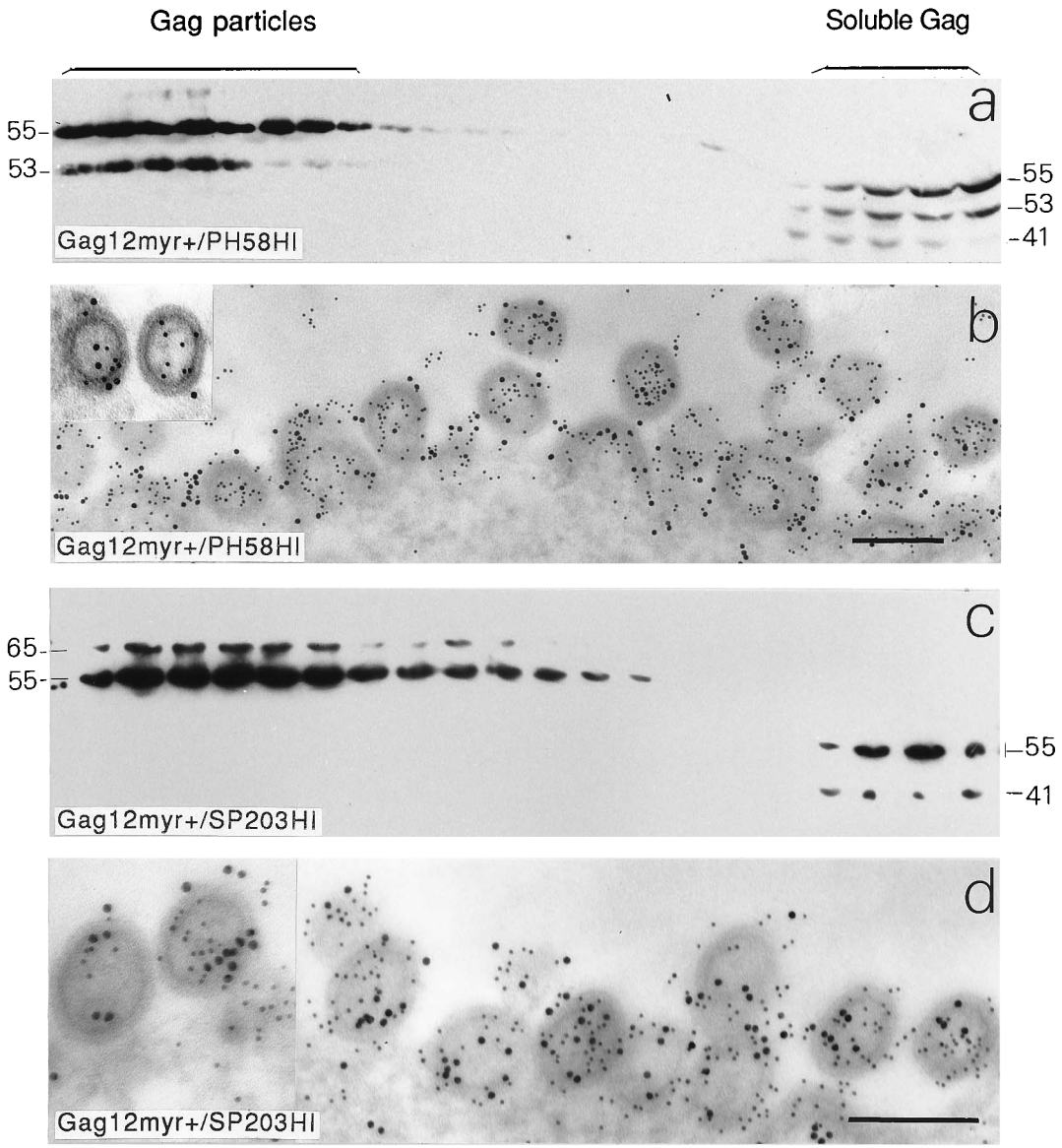

FIG. 6. *trans* rescue and coencapsidation of Gag chimeras by HIV-1 WT Pr55^{gag}. Sf9 cells were coinfected with Gag12myr+ (expressing WT Pr55^{gag}) and PH58HI (a and b) or Gag12myr+ and SP203HI chimera (b and d), and extracellular budding Gag particles were analyzed at 48 h postinfection by ultracentrifugation in a velocity gradient (a and c) and QIEM in double immunogold labeling (b and d). (a and c) Aliquots from the gradient fractions were analyzed by SDS-PAGE and immunoblotting with anti-Pr55-p24 MAb Epiclone-5001, peroxidase-labeled conjugate, and luminescent substrate. The positions of WT Pr55^{gag} (55 kDa), Gag chimeras PH58HI (53 kDa) and SP203HI (65 kDa), and cleavage products (Pr41^{gag}) are indicated at the sides. (b) Double immunolabeling with (i) anti-p6 rat MAb and 5-nm-gold-labeled anti-rat IgG conjugate (specific for HIV-1 Pr55^{gag}) and (ii) antipolyhedrin rabbit antibody and 10-nm-gold-labeled anti-rabbit IgG conjugate (specific for PH58HI). (d) Double labeling with (i) anti-HIV-1 MA mouse MAb Epiclone-5003 and 5-nm-gold-labeled anti-mouse IgG conjugate and (ii) anti-HSRV MA rabbit antibody and 10-nm-gold-labeled anti-rabbit IgG conjugate. Sharper contours for composite Gag particles were obtained by 3-min poststaining with lead acetate (insets). Bar, 200 nm.

results, and additional data from substitution mutagenesis of HIV-1 NC (10), confirmed the existence of a third major morphogenetic domain (AD3) in Gag, spanning the sp2-NC p7 junction and the cysteine-histidine boxes of HIV-1 NC (60, 61). However, the two Cys-His motifs did not seem to be directly involved in Gag-Gag interaction in HIV (2) and RSV (58).

The difference between N-myristylated and unmyristylated Gag amber mutants in relation to the regions critical for their *trans* rescue by WT Pr55^{gag} suggested that additional factors and parameters, other than the presence of interacting domains in the Gag proteins, e.g., Gag conformation, transport, or binding to cellular chaperons, could be involved in the observed phenomenon. In this hypothesis, the targeting of the N-myristylated Gag amber mutants to the plasma membrane would allow their concentration at the membrane sites of assembly and budding and coencapsidation with WT Pr55^{gag}, even through weak interactions, as in the case of *amb*143myr+ or *amb*209myr+. By contrast, transport-defective unmyristylated Gag species could reach the membrane budding sites only if they first establish bonds with WT Pr55^{gag}. In addition, the affinities of different domains of Gag amber mutants for their WT Pr55^{gag} partners would depend upon both their sequences and their conformations and thus be influenced by their N myristylation. The possible role of the cellular environ-

TABLE 3. Immunoreactivities of homogeneous and composite retrovirus-like core particles in EM sections of Sf9 cells expressing one or two Gag precursor species[a]

Recombinant expressed	Immunoreactivity with[b]:				Ratio[c]
	Anti-HIV p6	Antipolyhedrin	Anti-HIV p17	Anti-HRSV MA	
HIV-1 Pr55^{gag} alone					
Mb	16.61 ± 0.76 (287)	≤0.2	14.77 ± 1.04 (202)	≤0.2	
Cy	18.76 ± 1.12 (83)	≤0.2	15.73 ± 1.23 (66)	≤0.2	
Nu	22.62 ± 1.39 (104)	≤0.2	14.47 ± 0.84 (90)	≤0.2	
PH58HI alone					
Mb	≤0.2	ND[d]			
Cy	≤0.2	14.95 ± 0.84 (172)			
Nu	≤0.2	13.66 ± 2.07 (32)			
HIV-1 Pr55^{gag} + PH58HI					
Mb	19.87 ± 1.69 (93)	4.80 ± 0.67 (93)			4.14
Cy	19.57 ± 1.68 (47)	7.13 ± 1.12 (47)			2.74
Nu	13.28 ± 1.58 (90)	14.07 ± 1.99 (90)			0.94
SP203HI alone					
Mb			≤0.2	ND	
Cy			≤0.2	16.72 ± 1.23 (75)	
Nu			≤0.2	ND	
HIV-1 Pr55^{gag} + SP203HI					
Mb			20.89 ± 1.34 (113)	5.56 ± 0.70 (113)	3.75
Cy			14.10 ± 3.40 (22)	7.41 ± 2.12 (22)	1.90
Nu			ND	ND	

[a] Gag particles were examined by QIEM in different compartments (plasma membrane [Mb], cytoplasm [Cy], and nucleus [Nu]) of Sf9 cells harvested at 48 h after single (homogeneous particles) or double (composite particles) infection. Since N-myristylated HIV-1 WT Pr55^{gag} self-assembled at the plasma membrane, the reactivities of intracellular core particles were analyzed by using GagG2A, which expresses a myristylation-defective full-length Pr55^{gag} (6).

[b] Numbers of gold grains per Gag particle (mean ± confidence interval at the $P = 0.05$ level). Values in parentheses represent the number of Gag core particles analyzed. Background labeling varied between 0.1 and 0.2 grain per particle.

[c] Ratio of anti-p6 to antipolyhedrin or anti-HIV p17 (Epiclone-5003) to anti-HRSV MA, reactivity, expressed as number of colloidal gold grains per particle.

[d] ND, not detected. Retrovirus-like particles assembled by the PH58HI and SP203HI chimeras were never observed at the plasma membrane but only within the cell, in the cytoplasm (SP203HI), or in both the cytoplasm and the nucleus (PH58HI).

ment in Gag particle morphogenesis and coencapsidation process was examined by QIEM analysis of heterogeneous particles containing both HIV-1 WT Pr55^{gag} and an unmyristylated Gag chimera (Table 3). The results suggested that the number of copies of Gag chimera within composite particles, relative to HIV-1 WT Pr55^{gag}, significantly differed in intracellular and membrane-budding particles, implying that the intracellular transport and local concentration of different Gag protein species would influence the final composition of the assembling Gag particles.

The role of the MA domain in Gag interaction was indirectly explored by *trans*-rescue assays of Gag precursor species with the following MA modifications: (i) fusion to AcNPV polyhedrin sequence, as in PH58HI, (ii) substitution by another retroviral MA sequence from HSRV, as in the SP203HI chimera, or (iii) deletion of the entire MA domain, as in Pr39^{gag} produced by mutant *in*40 or *dl*42-100 (6, 7). Pr39^{gag} failed to be coencapsidated with WT Pr55^{gag}, suggesting that the CA-NC domains of HIV-1 could not form stable bonds with WT Pr55^{gag} in vivo in the absence of the MA domain. However, the Gag chimeras expressed by PH58HI and SP203HI were found to be coencapsidated with HIV-1 Pr55^{gag} in significant amounts (Table 1). The level of coencapsidation was higher for PH58HI, of which the N-terminal 14 amino acids from HIV-1 MA were substituted by a foreign sequence of 58 residues from the AcNPV polyhedrin, than for SP203HI, which contained an entire heterologous MA sequence of 203 residues from a spumaretrovirus. Considering the sequence of the baculovirus polyhedrin and the evolutionary divergence between the HIV and HSRV genomes, these results suggested a certain degree of tolerance for Gag particle assembly and release at the N terminus of the HIV-1 Gag precursor, in terms of MA length and amino acid sequence (11). This is consistent with two recent reports showing that RSV-HIV chimeras consisting of the carboxy-terminal moiety of HIV Gag protein fused to the amino-terminal moiety of an RSV Gag molecule are functional for Gag assembly and budding (2) and that the central HIV-1 MA domain is nonessential for Gag–β-galactosidase fusion protein coencapsidation (56). This notion has some implications for the construction of HIV-1 Gag fusion proteins designed for copackaging of foreign sequences (58, 59).

ACKNOWLEDGMENTS

This work was supported by the Agence Nationale de Recherche sur le SIDA (AC-14), the Centre National de la Recherche Scientifique, the Fondation pour la Recherche Médicale, and the Fédération des Groupements d'Entreprises Fraçaises dans la Lutte contre le Cancer.

We thank Saw See Hong for critical reading of the manuscript, Jeannette Tournier, Martine Bardy, and Nolwenn Coudronnière for technical contributions, and Liliane Cournud for secretarial aid.

REFERENCES

1. **Argos, P.** 1989. A possible homology between immunodeficiency virus p24 core protein and picornaviral VP2 coat protein: prediction of HIV p24 antigenic sites. EMBO J. **8:**779–785.
2. **Bennett, R. P., T. D. Nelle, and J. W. Wills.** 1993. Functional chimeras of the Rous sarcoma virus and human immunodeficiency virus Gag proteins. J. Virol. **67:**6487–6498.
3. **Blomberg, J., and P. Medstrand.** 1990. A sequence in the carboxylic termi-

nus of the HIV-1 matrix protein is highly similar to sequences in membrane-associated proteins of other RNA viruses: possible functional implications. New Biol. **2:**1044–1046.
4. **Bryant, M., and L. Ratner.** 1990. Myristoylation-dependent replication and assembly of human immunodeficiency virus 1. Proc. Natl. Acad. Sci. USA **87:**523–527.
5. **Burtonboy, G., M. Bodeus, N. Delferrière, M. Surleraux, A. Rovayo, V. Vercruyse, and J. C. Fang.** 1990. Rat monoclonal antibodies against viral antigen, p. 339–353. *In* H. Bazin (ed.), Rat hybridomas and rat monoclonal antibodies. CRC Press, Inc., Boca Raton, Fla.
6. **Chazal, N., C. Carrière, B. Gay, and P. Boulanger.** 1994. Phenotypic characterization of insertion mutants of the human immunodeficiency virus type 1 Gag precursor expressed in recombinant baculovirus-infected cells. J. Virol. **68:**111–122.
7. **Chazal, N., B. Gay, C. Carrière, J. Tournier, and P. Boulanger.** 1995. Human immunodeficiency virus type 1 MA deletion mutants expressed in baculovirus-infected cells: *cis* and *trans* effects on the Gag precursor assembly pathway. J. Virol. **69:**365–375.
8. **Craven, R. C., A. E. Leure-du-Pree, C. R. Erdie, C. B. Wilson, and J. W. Wills.** 1993. Necessity of the spacer peptide between CA and NC in the Rous sarcoma virus Gag protein. J. Virol. **67:**6246–6252.
9. **Defer, C., M. T. Belin, M. L. Caillet-Boudin, and P. Boulanger.** 1990. Human adenovirus-host cell interactions: a comparative study with members of subgroups B and C. J. Virol. **64:**3661–3673.
10. **Dorfman, T., J. Luban, S. P. Goff, W. A. Haseltine, and H. G. Göttlinger.** 1993. Mapping of functionally important residues of a cysteine-histidine box in the human immunodeficiency virus type 1 nucleocapsid protein. J. Virol. **67:**6159–6169.
11. **Dorfman, T., F. Mammano, W. A. Haseltine, and H. G. Göttlinger.** 1994. Role of the matrix protein in the virion association of the human immunodeficiency virus type 1 envelope glycoprotein. J. Virol. **68:**1689–1696.
12. **Ehrlich, L. S., B. E. Agresta, C. A. Gelfand, J. Jentoft, and C. A. Carter.** 1994. Spectral analysis and tryptic susceptibility ss probes of HIV-1 capsid protein structure. Virology **204:**515–525.
13. **Fäcke, M., A. Janetzko, R. L. Shoeman, and H.-G. Kräusslich.** 1993. A large deletion in the matrix domain of the human immunodeficiency virus *gag* gene redirects virus particle assembly from the plasma membrane to the endoplasmic reticulum. J. Virol. **67:**4972–4980.
14. **Franke, E. K., H. En Hui Yuan, K. L. Bossolt, S. P. Goff, and J. Luban.** 1994. Specificity and sequence requirements for interactions between various retroviral Gag proteins. J. Virol. **68:**5300–5305.
15. **Gelderblom, H. R.** 1991. Assembly and morphology of HIV: potential effect of structure on viral function. AIDS **5:**617–638.
16. **Gheysen, D., E. Jacobs, F. de Foresta, C. Thiriart, M. Francotte, D. Thines, and M. De Wilde.** 1989. Assembly and release of HIV-1 precursor Pr55^{gag} virus-like particles from recombinant baculovirus-infected insect cells. Cell **59:**103–112.
17. **Göttlinger, H. G., T. Dorfman, J. G. Sodroski, and W. A. Haseltine.** 1991. Effect of mutations affecting the p6 *gag* protein on human immunodeficiency virus particle release. Proc. Natl. Acad. Sci. USA **88:**3195–3199.
18. **Göttlinger, H. G., J. G. Sodroski, and W. A. Haseltine.** 1989. Role of capsid precursor processing and myristoylation in morphogenesis and infectivity of human immunodeficiency virus type 1. Proc. Natl. Acad. Sci. USA **86:**5781–5785.
19. **Guan, K. L., and J. E. Dixon.** 1991. Eukaryotic proteins expressed in *Escherichia coli*: an improved thrombin cleavage and purification procedure of fusion proteins with glutathione *S*-transferase. Anal. Biochem. **192:**262–267.
20. **Hendersson, L. E., M. A. Bowers, R. C. Sowder, S. A. Serabyn, D. G. Johnson, J. W. Bess, Jr., L. O. Arthur, D. K. Bryant, and C. Fenselau.** 1992. Gag proteins of the highly replicative MN strain of human immunodeficiency virus type 1: posttranslational modifications, proteolytic processing, and complete amino acid sequences. J. Virol. **66:**1856–1865.
21. **Hong, S. S., and P. Boulanger.** 1993. Assembly-defective point mutants of the immunodeficiency virus type 1 Gag precursor phenotypically expressed in recombinant baculovirus-infected cells. J. Virol. **67:**2787–2798.
22. **Hughes, B. P., T. F. Booth, A. S. Belyaev, D. McIlroy, J. Jowett, and P. Roy.** 1993. Morphogenic capabilities of human immunodeficiency virus type 1 Gag and *gag-pol* proteins in insect cells. Virology **193:**242–255.
23. **Jacks, T., M. D. Power, F. R. Masiarz, P. A. Luciw, P. J. Barr, and H. E. Varmus.** 1988. Characterization of ribosomal frame-shift in HIV-1 gag-pol expression. Nature (London) **331:**280–283.
24. **Jowett, J. B. M., D. J. Hockley, M. V. Nermut, and I. M. Jones.** 1992. Distinct signals in HIV-1 Pr55 necessary for RNA binding and particle formation. J. Gen. Virol. **73:**3079–3086.
25. **Karayan, L., B. Gay, J. Gerfaux, and P. Boulanger.** 1994. Oligomerization of recombinant penton base of adenovirus type 2 and its assembly with fiber in baculovirus-infected cells. Virology **202:**782–795.
26. **Laemmli, U. K.** 1970. Cleavage of structural proteins during the assembly of the head of bacteriophage T4. Nature (London) **227:**680–685.
27. **Langedijk, J. P. M., J. J. Schalken, M. Tersmette, J. G. Huisman, and R. H. Meloen.** 1990. Location of epitopes on the major core protein p24 of human immunodeficiency virus. J. Gen. Virol. **71:**2609–2614.
28. **Layne, S. P., M. J. Merges, M. Dembo, J. L. Spouge, S. R. Conley, J. P. Moore, J. L. Raina, H. Renz, H. R. Gelderblom, and P. L. Nara.** 1992. Factors underlying spontaneous inactivation and susceptibility to neutralization of human immunodeficiency virus. Virology **189:**695–714.
29. **Löchelt, M., H. Zentgraf, and R. Flügel.** 1991. Construction of an infectious DNA clone of the full-length human spumaretrovirus genome and mutagenesis of the *bel*-1 gene. Virology **184:**43–54.
30. **Luban, J., K. L. Bossolt, E. K. Franke, G. V. Kalpana, and S. P. Goff.** 1993. Human immunodeficiency virus type 1 gag protein binds to cyclophilins A and B. Cell **73:**1067–1078.
31. **Luban, J., C. Lee, and S. P. Goff.** 1993. Effect of linker insertion mutations in the human immunodeficiency virus type 1 *gag* gene on activation of viral protease expressed in bacteria. J. Virol. **67:**3630–3634.
32. **Luckow, V. A., and M. D. Summers.** 1989. High level expression of nonfused foreign genes with *Autographa californica* nuclear polyhedrosis virus expression vectors. Virology **170:**31–39.
33. **Mammano, F., Å. Öhagen, S. Höglund, and H. G. Göttlinger.** 1994. Role of the major homology region of human immunodeficiency virus type 1 in virion morphogenesis. J. Virol. **68:**4927–4936.
34. **Mervis, R. J., N. Ahmad, E. P. Lillehoj, M. G. Raum, F. H. R. Salazar, H. W. Chan, and S. Venkatesan.** 1988. The *gag* gene products of human immunodeficiency virus type 1: alignment within the *gag* open reading frame, identification of posttranslational modifications, and evidence for alternative Gag precursors. J. Virol. **62:**3993–4002.
35. **Niedrig, M., H. S. Gelderblom, G. Pauli, J. März, H. Bickhardt, H. Wolf, and S. Modrow.** 1994. Inhibition of infectious human immunodeficiency virus type 1 particle formation by Gag protein-derived peptides. J. Gen. Virol. **75:**1469–1474.
36. **Novelli, A., and P. Boulanger.** 1991. Deletion analysis of functional domains in baculovirus-expressed adenovirus type 2 fiber. Virology **185:**365–376.
37. **Overton, H. A., Y. Fuji, I. R. Price, and I. M. Jones.** 1989. The protease and gag gene products of the human immunodeficiency virus: authentic cleavage and post-translational modification in an insect cell expression system. Virology **170:**107–116.
38. **Pal, R., M. S. Reitz, Jr., E. Tschachler, R. C. Gallo, M. G. Sarngadharan, and F. D. M. Veronese.** 1990. Myristoylation of *gag* polyproteins of HIV-1 plays an important role in virus assembly. AIDS Res. Hum. Retroviruses **6:**721–730.
39. **Park, J., and C. D. Morrow.** 1992. The nonmyristylated Pr160$^{gag\text{-}pol}$ polyprotein of human immunodeficiency virus type 1 interacts with Pr55^{gag} and is incorporated into viruslike particles. J. Virol. **66:**6304–6313.
40. **Rein, A., M. R. McClure, N. R. Rice, R. B. Luftig, and A. M. Schultz.** 1986. Myristylation site in Pr65^{gag} is essential for virus particle formation by Moloney murine leukemia virus. Proc. Natl. Acad. Sci. USA **83:**7246–7250.
41. **Robert-Hebmann, V., S. Emiliani, F. Jean, M. Resnicoff, F. Traincard, and C. Devaux.** 1992. Clonal analysis of murine B-cell response to the human immunodeficiency virus type 1 (HIV-1) *gag* p17 and p25 antigens. Mol. Immunol. **29:**729–738.
42. **Royer, M., M. Cerutti, B. Gay, S. S. Hong, G. Devauchelle, and P. Boulanger.** 1991. Functional domains of HIV-1 *gag*-polyprotein expressed in baculovirus-infected cells. Virology **184:**417–422.
43. **Royer, M., S. S. Hong, B. Gay, M. Cerutti, and P. Boulanger.** 1992. Expression and extracellular release of human immunodeficiency virus type 1 Gag precursors by recombinant baculovirus-infected cells. J. Virol. **66:**3230–3235.
44. **Sanger, F., S. Nicklen, and A. R. Coulson.** 1977. DNA sequencing with chain-terminating inhibitors. Proc. Natl. Acad. Sci. USA **74:**5463–5467.
45. **Schultz, A. M., and A. Rein.** 1989. Unmyristylated Moloney murine leukemia virus Pr65^{gag} is excluded from virus assembly and maturation events. J. Virol. **63:**2370–2373.
46. **Smith, A. J., N. Srinivasakumar, M. L. Hammarskjöld, and D. Rekosh.** 1993. Requirements for incorporation of Pr160$^{gag\text{-}pol}$ from human immunodeficiency virus type 1 into virus-like particles. J. Virol. **67:**2266–2275.
47. **Spearman, P., J.-J. Wang, N. Vander Heyden, and L. Ratner.** 1994. Identification of human immunodeficiency virus type 1 Gag protein domains essential to membrane binding and particle assembly. J. Virol. **68:**3233–3242.
48. **Strambio-de-Castillia, C., and E. Hunter.** 1992. Mutational analysis of the major homology region of Mason-Pfizer monkey virus by use of saturation mutagenesis. J. Virol. **66:**7021–7032.
49. **Tanchou, V., T. Delaunay, H. de Rocquigny, M. Bodeus, J. L. Darlix, B. Roques, and R. Benarous.** 1994. Monoclonal antibody-mediated inhibition of RNA binding and annealing of human immunodeficiency virus type 1 nucleocapsid protein of the AIDS Res. Hum. Retroviruses **10:**983–993.
50. **Trono, D., M. B. Feinberg, and D. Baltimore.** 1989. HIV-1 Gag mutants can dominantly interfere with the replication of the wild-type virus. Cell **59:**113–120.
51. **Veronese, F. D. M., R. Rahman, T. D. Copeland, S. Oroszlan, R. C. Gallo, and M. G. Sarngadharan.** 1987. Immunological and chemical analysis of p6, the carboxyl-terminal fragment of HIV p15. AIDS Res. Hum. Retroviruses **3:**253–264.
52. **Von Poblotzki, A., R. Wagner, M. Niedrig, G. Wanner, H. Wolf, and S. Modrow.** 1993. Identification of a region in the Pr55*gag*-polyprotein essential for HIV-1 particle formation. Virology **193:**981–985.

53. **Wagner, R., L. Deml, H. Fließbach, G. Wanner, and H. Wolf.** 1994. Assembly and extracellular release of chimeric HIV-1 $Pr55^{gag}$ retrovirus-like particles. Virology **200:**162–175.
54. **Wain-Hobson, S., P. Sonigo, O. Danos, S. Cole, and M. Alizon.** 1985. Nucleotide sequence of the AIDS virus, LAV. Cell **40:**9–17.
55. **Wang, C.-T., and E. Barklis.** 1993. Assembly, processing, and infectivity of human immunodeficiency virus type 1 Gag mutants. J. Virol. **67:**4264–4273.
56. **Wang, C.-T., J. Stegeman-Olsen, Y. Zhang, and E. Barklis.** 1994. Assembly of HIV GAG-β-galactosidase fusion proteins into virus particles. Virology **200:**524–534.
57. **Weldon, R. A., Jr., C. R. Erdie, M. G. Oliver, and J. W. Wills.** 1990. Incorporation of chimeric Gag protein into retroviral particles. J. Virol. **64:**4169–4179.
58. **Weldon, R. A., Jr., and J. W. Wills.** 1993. Characterization of a small (25-kilodalton) derivative of the Rous sarcoma virus Gag protein competent for particle release. J. Virol. **67:**5550–5561.
59. **Wills, J. W.** 1989. Retro-secretion of recombinant proteins. Nature (London) **340:**323–324.
60. **Wills, J. W., C. E. Cameron, C. B. Wilson, Y. Xiang, R. P. Bennett, and J. Leis.** 1994. An assembly domain of the Rous sarcoma virus Gag protein required late in budding. J. Virol. **68:**6605–6618.
61. **Wills, J. W., and R. C. Craven.** 1991. Form, function, and use of retroviral gag proteins. AIDS **5:**639–654.
62. **Wills, J. W., R. C. Craven, R. A. Weldon, Jr., T. D. Nelle, and C. R. Erdie.** 1991. Suppression of retroviral MA deletions by the amino-terminal membrane-binding domain of $p60^{src}$. J. Virol. **65:**3804–3812.
63. **Yu, X. F., Q. C. Yu, T. H. Lee, and M. Essex.** 1992. The C terminus of human immunodeficiency virus type 1 matrix protein is involved in early steps of the virus life cycle. J. Virol. **66:**5667–5670.
64. **Yu, X. F., X. Yuan, Z. Matsuda, T. H. Lee, and M. Essex.** 1992. The matrix protein of human immunodeficiency virus type 1 is required for incorporation of viral envelope protein into mature virions. J. Virol. **66:**4966–4971.
65. **Yuan, X., X. F. Yu, T. H. Lee, and M. Essex.** 1993. Mutations in the N-terminal region of human immunodeficiency virus type 1 matrix protein block intracellular transport of the Gag precursor. J. Virol. **67:**6387–6394.
66. **Zhao, Y., I. M. Jones, D. J. Hockley, M. V. Nermut, and P. Roy.** 1994. Complementation of human immunodeficiency virus type 1 (HIV-1) Gag particle formation. Virology **199:**403–408.
67. **Zhou, W., L. J. Parent, J. W. Wills, and M. D. Resh.** 1994. Identification of a membrane-binding domain within the amino-terminal region of human immunodeficiency virus type 1 Gag protein which interacts with acidic phospholipids. J. Virol. **68:**2556–2569.